JOURNAL OF AIRCRAFT
Vol. 47, No. 1, January–February 2010

Probabilistic Sensitivity-Based Ranking of Damage Tolerance Analysis Elements

Harry R. Millwater*
University of Texas at San Antonio, San Antonio, Texas 78249
and
David H. Wieland†
Southwest Research Institute, San Antonio, Texas 78238

DOI: 10.2514/1.44498

A damage tolerance analysis contains a number of elements such as expected usage, structural and fatigue-related material properties, crack size, geometry, stress intensity factor, retardation model and constants, and others. Understanding of the relative significance of these elements is integral to performing a successful damage tolerance analysis and determining future research efforts to improve the accuracy of damage tolerance analysis. These elements have associated with them inherent uncertainty (as in material properties) or statistical uncertainty (as in loads, initial crack sizes, and geometry). Also, the assumptions contained in the analysis methods may result in modeling errors, that is, the use of simplified models to represent complex behavior. In this research, the relative significance of the elements of a damage tolerance analysis were calculated and ranked from a probabilistic sensitivity standpoint. The expected variation of damage tolerance analysis inputs, for example, initial crack size, fracture toughness, hole size, etc., were modeled with probability distributions determined from experimental tests and aircraft or component teardowns. Discrete parameters such as the retardation model were varied through discrete changes to the model and reanalysis. The probabilistic sensitivities, the derivative of the probability of failure with respect to statistical moments (mean, standard deviation), were determined using Monte Carlo sampling and used as the metric to rank the importance of the damage tolerance analysis elements. The methodology was applied through a numerical analysis to a fatigue critical location of a T-38 wing considering three different usages ranging from severe to mild.

Nomenclature

C	=	Paris coefficient
E	=	expected value operator
f_X	=	probability density function
$g(\mathbf{x})$	=	limit state; $g \leq 0$ denotes failure
$I(\mathbf{x})$	=	indicator function; $I = 1$ denotes failure
K_c	=	thickness-dependent fracture toughness
K_{Ic}	=	plane strain fracture toughness
M_f	=	number of failure points during Monte Carlo sampling
M_{tot}	=	total number of Monte Carlo samples
m	=	Walker equation constant
N	=	flight hours
N_f	=	computed flight hours to failure
N_o	=	user-specified number of cycles
n	=	Paris exponent
P_f	=	probability of failure
R	=	stress ratio (min/max load)
S_μ	=	normalized and nondimensionalized sensitivity with respect to mean
S_σ	=	normalized and nondimensionalized sensitivity with respect to standard deviation
χ	=	comparison index for discrete variables
Γ_{μ_i}	=	sensitivity of failure probability with respect to mean value of random variable i, $\frac{\partial P}{\partial \mu_i}$
Γ_{σ_i}	=	sensitivity of failure probability with respect to standard deviation of random variable i, $\frac{\partial P}{\partial \mu_i}$
κ	=	kernel function for sensitivity calculations
μ	=	mean value
σ	=	standard deviation
σ_{ys}	=	yield stress

Presented as Paper 1836 at the 44th AIAA/ASME/ASCE/AHS/ASC Structures, Structural Dynamics, and Materials Conference, Norfolk, VA, 7–10 April 2003; received 20 March 2009; revision received 13 September 2009; accepted for publication 16 September 2009.

*Associate Professor, Mechanical Engineering, One UTSA Circle. Member AIAA.
†Principal Engineer, 6220 Culebra Road. Member AIAA.

I. Introduction

THE U.S. Air Force has been using damage tolerance analysis (DTA) methods since the early 1970s to design new aircraft and determine inspection intervals for aging aircraft. New aircraft are designed using DTA such that a rogue flaw in the structure will not grow to failure between inspections [1]. Aircraft that were designed before the widespread use of DTA methods have been reanalyzed using DTA methods to determine inspection intervals to ensure safety of flight.

A DTA contains a number of elements such as expected usage, usage-to-stress models, structural and fatigue-related material properties, crack size, geometry, stress intensity factor, retardation model constants, and others. Understanding of the relative significance of these elements is integral to performing a successful DTA and determining future research efforts to improve the DTA. These elements have associated with them inherent uncertainty (as in material properties) or statistical uncertainty (as in loads, initial crack sizes, and geometry). Also, the assumptions contained in the analysis methods may result in modeling errors, that is, the use of simplified models to represent complex behavior.

Probabilistic damage tolerance methods (PDTA) are ideally suited to account formally for the variations of inputs using probability distributions, a probability of failure estimate, and probabilistic sensitivities. A fundamental component of PDTA is accurate characterizations of the probability distributions. This information is often difficult to obtain. As such, probabilistically based sensitivity

measures can provide information useful to determining the significant elements of the PDTA and can suggest the optimum approach to improve the PDTA.

There are a number of previous approaches to a probabilistic DTA and an aircraft risk assessment. Yang [2] and Yang and Manning [3–5] have a series of papers describing the development and application of a lognormal random process to stochastic crack growth of airframe structure. This methodology uses a single random variable to encompass the variations in fatigue crack growth rate. The method is straightforward to apply and uses any existing deterministic fatigue crack growth prediction. However, the various elements of a DTA are not characterized probabilistically.

Lincoln [6,7] applied risk assessment methods to the aging U.S. Air Force fleet. Risk assessments have been performed for the B-52 wing, KC-135 wing, C-5A wing, C-141B fuselage and wing, F-5 fuselage, T-38 fuselage and wing, and T-37 complete aircraft. One use for risk assessments is the situation in which a potential cracking problem has been revealed and the aircraft are beyond their deterministic damage tolerance limits. As such, a risk assessment may be used to provide a basis for continued flight until the required inspections can be performed or as a basis for determining modified inspection intervals.

Berens et al. [8], Berens and Loomis [9], and Miedlar et al. [10] have developed and enhanced the probability of fracture (PROF) risk assessment computer code. PROF computes the probability of fracture versus flight hours associated with a fatigue critical location (FCL) considering inspection, repair, and replacement at the aircraft, airframe, or fleet level. Required input data consist of the initial crack size distribution, crack size versus time, stress intensity geometry correction factor, fracture toughness, extreme value distribution of maximum stress per flight, inspection times, probability of detection curves, and repair crack size distributions. Probabilistic sensitivity results are not an output of the program but may be computed through parameter studies requiring reanalysis. PROF has been applied to develop risk predictions for a number of military aircraft; see [11] for an analysis of an F-5 aircraft.

A seven-stage probabilistic pitting corrosion fatigue life model from pit nucleation through fracture has been developed that is applicable to aircraft structure [12]. The structure analyzed was that of an infinite plate with a circular rivet hole constructed of aluminum alloy 2024-T3 with a single nucleation site. Mean values were determined from data. The distribution functions were assumed and the coefficient of variations assumed then varied. Probabilistic sensitivity analysis was computed and indicated that the pit nucleation time and the material constant for small crack growth were the two most important random variables.

Rusk et al. [13] combined probabilistic damage tolerance methods with Bayesian updating to determine the probability distribution of damage sizes in composites using aircraft service inspection defect data in airframe composites. In this research, Bayesian updating techniques were used to revise initial estimates of damage size distributions using composite damage size data from the Federal Aviation Administration's Service Difficulty Reporting System database. In nearly every case, the results showed that the baseline distributions are a conservative estimate of the range of damage sizes encountered on commercial composite structural applications.

McGinty [14] discussed the sensitivities of DTA elements by examining the deterministic ratio of the percent change of input to the percent change of output, that is, the nondimensionalized derivative of the governing equation. The following studies were developed: 1) the sensitivity of the stress intensity factor to the stress intensity geometry correction factor (beta), stress, and crack size; 2) the sensitivity of the crack growth rate to beta, Paris coefficient, Paris exponent, and crack size; and 3) the sensitivity of the fatigue life to beta, Paris coefficient, Paris exponent, and initial and final crack sizes. The results indicate that the geometry correction factor (beta) and the applied stress are the important factors with respect to fatigue life. These studies are informative; however, there was no consideration for the amount of variation that might be expected in any parameter.

Fawaz and Harter [15] studied the impact of various parameters on DTA estimates using deterministic parameter studies. The expected variation in the parameters was estimated using engineering judgment. Each parameter was varied one at a time; thus, there were no interaction effects included. The cycles to failure was used as a metric of importance. Five different cracking scenarios were studied of a transport aircraft fuselage crack scenario under remote tension: a single through crack at a hole, a double through crack at a hole, a single corner crack at a hole, a double corner crack at a hole, and a double oblique through crack at a hole. The material properties and their variation were chosen as representative of a 2024-T3 aluminum sheet. Eight parameters were deemed important and, per the analysis results, divided into first- and second-order effects. The first-order parameters were the initial flaw size assumption, geometry correction factor, load interaction models, crack growth rate data, and stress intensity factor. The secondary parameters were the yield stress, fracture toughness, and threshold stress intensity factor. The distinction between the first- and second-order effects was based on whether the life-cycle costs could be reduced via a more appropriate inspection schedule or if flight safety was affected. The parameters within each category are not comparatively ranked.

The approach implemented in this research was to explicitly compute probabilistic sensitivity factors, $\partial P/\partial \mu_i$ and $\partial P/\partial \sigma_i$, that is, the derivatives of the probability of failure with respect to the mean and standard deviation of the input parameters, and to use these factors, once nondimensionalized, as a metric for determining the relative importance of the various DTA elements. The advantages of this approach are several. First, the analysis and metrics are probabilistically based and the probability density functions of the random variables were explicitly modeled, supported by a significant amount of test data. Therefore, the amount of variation of a variable and its likelihood were modeled explicitly through the probability density functions. Second, random sampling was implemented such that all combinations of variables were considered according to their probability density functions; thus, interaction effects were included. Third, the metrics consider the sensitivity of the mean and standard deviation separately, thus delineating the importance of each. Fourth, these results provide a means to make design-improvement cost decisions, for example, the amount of reduction in the probability of failure obtainable if the mean hole diameter is reduced by a given percentage.

The probabilistic sensitivity approach to DTA is demonstrated using a fatigue critical location of a T-38 wing. The T-38 was chosen because it is a highly maneuverable aircraft with a large amount of data available. Thirteen random variables and three discrete variables were modeled with the random variable distributions developed from test data. The three usages examined were 1) Introduction to Fighter Fundamental (IFF), Supplemental Undergraduate Pilot Training (SUPT), and Astronaut Proficiency and Shuttle Training (NASA). These usages range from severe to mild, respectively. The analysis was supported by a detailed development of the random variable distributions based on teardowns and material property tests.

Section II describes the probabilistic damage tolerance methodology, particularly the probabilistic sensitivity measures. Section III describes the DTA model for the fatigue critical location of interest. Subsequently, the random variable development is described with supporting data and figures. Section IV discusses the results of the probabilistic sensitivity analyses. Section V discusses the effects of discrete variables, followed by discussion in Sec. VI and conclusions in Sec. VII.

II. Probabilistic Damage Tolerance Analysis Methodology

Probabilistic DTA involves the computation of the probability of failure (POF) of an FCL subject to a spectrum loading. The POF is determined mathematically as the integral of the joint probability density function over the failure domain, that is,

$$P_f = \int_{g(\mathbf{x},N)\le 0} f_{\mathbf{x}}(\mathbf{x})\,\mathrm{d}\mathbf{x} \tag{1}$$

where $\mathbf{X}$ denotes a vector of random variables,

$$d\mathbf{x} = \prod_{i=1}^{\text{nrv}} dx_i$$

$f_{\mathbf{x}}$, is the joint probability density function of the random variables, g denotes the limit state, and N denotes the computed number of flight hours to failure. The integral in Eq. (1) has the dimension of the number of random variables (nrv). The failure domain is defined by the limit state such that $g(\mathbf{X}, N) \leq 0$ denotes failure. For a DTA, g is defined as $g(\mathbf{X}, N_o) = N_f - N_o$, where N_o denotes a user-specified number of cycles and N_f the number of flight hours to fracture. Fracture is defined as $K_I(N) \geq K_C$, where K_I is the computed mode I stress intensity factor and K_C is the fracture toughness.

Equation (1) may be written in terms of an "indicator" function; $I(\mathbf{x})$ is defined such that

$$\text{failure: } I = 1 \quad \text{for } g \leq 0 \qquad \text{safe: } I = 0 \quad \text{for } g > 0 \quad (2)$$

Equation (1) becomes

$$P_f = \int_{-\infty}^{\infty} I(\mathbf{x}) f_{\mathbf{x}}(\mathbf{x})\, d\mathbf{x} = E[I(\mathbf{x})] \quad (3)$$

where E denotes the expected value operator.

The joint probability density function (PDF) for independent random variables is the product of the individual probability density functions,

$$f_{\mathbf{x}} = \prod_{i=1}^{\text{nrv}} f_{Xi} \quad (4)$$

The PDFs $f_{\tilde{X}i}$ are represented by commonly used distributions such as normal, lognormal, exponential, Weibull, extreme value, etc. [16]. Selection of the probability distribution type and its associated parameters, for example, mean and standard deviation, should be based on a statistical analysis of available or similar data. There are a number of statistical methods that can be used to select the appropriate distribution such as chi square [17], Kolmogorov–Smirnov [18], and Anderson–Darling [19], and others.

Equation (1) may be evaluated with a variety of probabilistic methods such as Monte Carlo sampling [20], importance sampling [20], first/second-order method [21], advanced mean value [22], and others. In this research, Monte Carlo sampling (MCS) was used, as this method is the most robust and the computational time for this study was not excessive. MCS involved computing repeated realizations of the random variables and evaluation of the limit state. The POF was estimated by the ratio of the number of failure points divided by the total number of samples as

$$P_f = E[I(\mathbf{x})] \approx \frac{1}{M_{\text{tot}}} \sum_{j=1}^{M_{\text{tot}}} I(\mathbf{x}_j) = \frac{M_f}{M_{\text{tot}}} \quad (5)$$

where M_{tot} is the total number of samples, and M_f is the number of samples for which $g(\mathbf{X}, N_o) \leq 0$. P_f is an estimate of the probability of failure. The variance of P_f and an associated confidence bound can be determined [23]. A POF can be computed for any particular N_o. N_o can be varied to obtain a cumulative distribution function of cycles to failure.

One method to determine the relative importance of the DTA variables is to use probabilistic sensitivity factors. Probabilistic sensitivity factors for a random variable are defined here in terms of the derivatives of the probability of failure with respect to the parameters of the input distribution, for example, $\partial P_f/\partial \mu_i$, $\partial P_f/\partial \sigma_i$, where μ_i and σ_i are the mean and standard deviation of the input random variable i. These sensitivities are then nondimensionalized to yield

$$\hat{S}_{\mu_i} = \frac{\partial P_f}{\partial \mu_i}\mu_i \qquad \hat{S}_{\sigma_i} = \frac{\partial P_f}{\partial \sigma_i}\sigma_i \quad (6)$$

Sensitivities of the probability of failure with respect to the mean and standard deviation of the random variables for independent random variables may be obtained by taking the derivative of Eq. (3) as [24,25]

$$\frac{\partial P}{\partial \theta_i} = \int_{-\infty}^{\infty} \left(I(\mathbf{x}) \frac{\partial f_{X_i}(x_i)}{\partial \theta_i} \frac{1}{f_{X_i}(x_i)} \right) f_{\mathbf{x}}(\mathbf{x})\, d\mathbf{x} = E[I(\mathbf{x})\kappa_{\theta_i}(\mathbf{x})] \quad (7)$$

where θ represents the mean or standard deviation.

κ is a kernel function defined generically as

$$\kappa_\theta = \frac{\partial f_X(x)}{\partial \theta} \cdot \frac{1}{f_X(x)} = \frac{\partial\, \ell_n[f]}{\partial \theta} \quad (8)$$

κ is distribution and parameter specific and is derived analytically for each distribution. Examples of kernel functions for a variety of probability distributions are given by Millwater [26].

The sensitivities can be estimated using the same samples that were used to estimate P_f as

$$\frac{\partial P_f}{\partial \theta_i} = E[I(\mathbf{x})\kappa_{\theta_i}] \approx \frac{1}{M_{\text{tot}}} \sum_{j=1}^{M_{\text{tot}}} I(X_j)\kappa_{\theta_i}(\mathbf{x}_j) \quad (9)$$

where $\mathbf{X}_j$ denotes the jth realization of the random variables. Thus, minimal additional computations are required once the probability of failure has been estimated.

It is convenient to organize the sensitivities as vectors, for example, $\{\hat{S}_{\mu_1}, \hat{S}_{\mu_2}, \ldots, \hat{S}_{\mu_{\text{nrv}}}\}$ and $\{\hat{S}_{\sigma_1}, \hat{S}_{\sigma_2}, \ldots, \hat{S}_{\sigma_{\text{nrv}}}\}$, and to normalize the vectors based on the L_2 norm ($\|\mathbf{S}\|_2 = \sqrt{S_1^2 + \cdots + S_N^2}$) such that the norm of the sensitivity vectors are "one." Normalized and nondimensionalized sensitivities S_{μ_i} and S_{σ_i} are developed as

$$S_{\theta_i} = \frac{\hat{S}_{\theta_i}}{\sqrt{\sum_{i=1}^{\text{nrv}} (\hat{S}_{\theta_i})^2}} \quad (10)$$

where θ denotes μ or σ. Also, because

$$\sum_{i=1}^{\text{nrv}} (S_{\theta_i})^2 = 1$$

$S_{\theta_i}^2$ can be considered as a percent contribution.

To compare results from different discrete analyses, that is, a discrete variable or option is changed and the POF and probabilistic sensitivities are determined, a dimensionless "comparison index," χ, is used consisting of the dot product of the vectors $\mathbf{S}_\theta$ from two solutions, that is,

$$\chi_\theta^{AB} = \mathbf{S}_\theta^{\text{discrete}A} \bullet \mathbf{S}_\theta^{\text{discrete}B} = \sum_{i=1}^{\text{nrv}} S_{\theta_i}^{\text{discrete}A} S_{\theta_i}^{\text{discrete}B} \quad (11)$$

A comparison index near one indicates the results of the two solutions are very similar and the discrete variable does not have a large effect on the ranking of the random variable sensitivities. Conversely, a value of χ significantly different from one indicates that the discrete variable has a significant effect. Note, however, that χ only examines the relative ranking of the sensitivities. The discrete variable might affect the absolute value of the mean or standard deviation of flight hours to failure, which is not covered by χ and must be evaluated by observing the changes in the mean and standard deviation directly.

The score function method is an exact formulation. The approximation arises in the calculation of the sensitivity integral, which is approximated here using Monte Carlo sampling; see Eq. (9). Therefore, sufficient samples must be used to ensure convergence of the sensitivities.

III. Damage Tolerance Analysis Model

The fatigue critical location evaluated was FCL A-15, a countersunk fastener hole in the lower wing skin at wing station 64.8 and the 15% spar. It is stressed primarily by the wing bending moment. The crack is assumed to grow from the base of the countersink

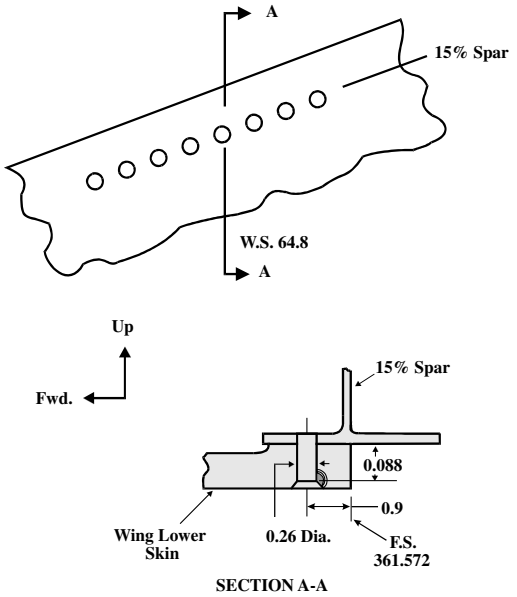

Fig. 1 FCL A-15 countersunk fastener hole at wing station 64.8 and 15% spar.

fastener hole to the free edge. The initial rogue flaw is approximated as a quarter-elliptical corner flaw; see Fig. 1.

A large amount of actual aircraft usage data was available for use on this project. Three different spectra were chosen to give a large variation in the usage stress spectra. The NASA usage [27] was chosen as a very mild usage, the SUPT usage[‡] was chosen as an average usage, and the IFF usage [28] was chosen as a severe usage. Figure 2 is a normal load factor exceedance diagram comparison of the three usages. FCL A-15 stress spectra were developed for each usage. The maximum spectrum stress was 18.2, 22.1, and 21.7 ksi for the NASA, SUPT, and IFF usage, respectively.

The material data (yield strength, plane strain fracture toughness, crack growth rate) were developed from various tests performed on 7075-T735 aluminum over a few decades [29–31]. Test data for thickness-dependent fracture toughness for the thickness of interest were not available; therefore, the equations in the NASGRO™ manual [32] for estimating the thickness-dependent fracture toughness as a function of the material yield strength and plane strain fracture toughness was used as follows:

$$K_C/K_{IC} = 1 + B_k e^{-(A_k t/t_0)} \qquad t_0 = 2.5(K_{IC}/\sigma_{ys})^2 \tag{12}$$

where A_k and B_k are constants, t represents sheet thickness, and σ_{ys} denotes the yield stress.

The crack growth rate data, da/dN versus ΔK, was developed from 448 test points at various R ratios. A segmented Walker equation for $R \geq 0$ was used of the form

$$\frac{da}{dN} = C[\Delta K(1-R)^{(m-1)}]^n \tag{13}$$

where C, m, and n are empirically derived material constants. The Walker equation was used to collapse the da/dN data for different R ratios down to a single curve, shown in Fig. 3, by using an m value of 0.57 and an R ratio cutoff value of 0.67. The R ratio cutoff value equaled the minimum of R (actual) and R (cutoff). Because there was a kink in the collapsed data, a three-segmented Walker equation was used; n was equal to 2.5, 4.6, or 3.15 for the first, second, and third segments, respectively. Two different retardation models, Willenborg [33] and Closure [34], were used with the spectrum-dependent constants developed from tests.

[‡]Private communication with J. Dubke, San Antonio Air Logistics Center Aircraft Directorate, Aircraft Structural Integrity Branch, dated 1 December 1994, subject "T-38 AETC Flight Loads Data Recording for the SUPT Usage," SwRI Project Number 06-5898.

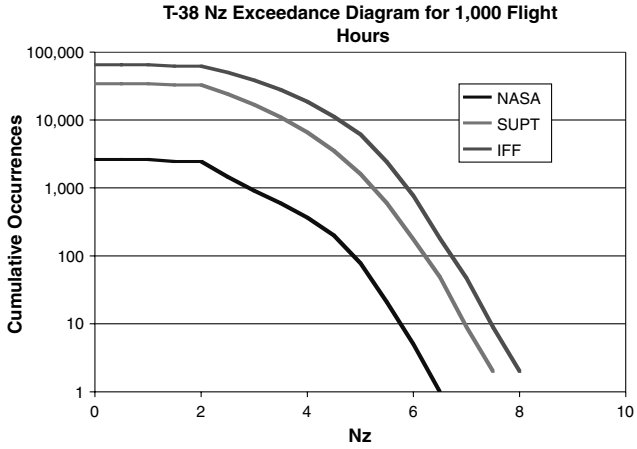

Fig. 2 T-38 normal load factor exceedance diagram.

A critical component to performing a meaningful probabilistic analysis is to determine the probability distribution type and parameters for a given random variable. The probability of failure and the probabilistic sensitivity results will be dependent in general on the probability distributions selected. Therefore, careful attention was paid to developing random variable distributions of DTA elements based on experimental tests and teardowns. However, it is known that probabilistic sensitivities are invariant to distribution type when computing sensitivities of the mean or standard deviation of the response (cycles to failure) if the input and outputs can be modeled reasonably by a quadratic (or linear) relationship [26]. In this example, the quadratic model is a good approximation ($R^2 = 0.91$); therefore, the rankings using probabilistic sensitivities of the median as a metric should be largely insensitive to the type of probability distribution, for example, normal vs Weibull, given the same mean and standard deviation for the input variables.

The potential random variables are any loading, geometric, fracture mechanics, and material properties. The decision whether to model a variable deterministically or probabilistically depends upon the relative importance of the variable on the POF. This importance depends upon, in general, the deterministic sensitivity and the amount of scatter of the random variable. Thus, variables with either a high deterministic sensitivity or large scatter or both are good candidates to be modeled as a random variable. If there is doubt, a logical approach is to model the variable probabilistically and let the analysis determine the relative importance.

The variations in input parameters consisted of continuous random variables modeled by probability distributions, such as initial crack size, and others that were discrete step changes, such as whether or not to model a countersink at the FCL fastener location. The variations of the continuous random variables were handled by formal probabilistic methods. Variations in the discrete variables were handled by repeated analyses with a discrete change in the affected variable.

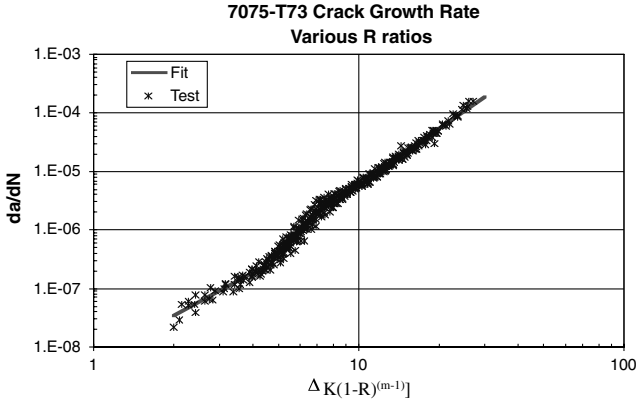

Fig. 3 Collapsed crack growth rate data and fit.

The continuous random variables were rogue flaw size, crack aspect ratio, stress intensity geometry factor (beta), yield strength, plane strain fracture toughness, thickness-dependent fracture toughness, crack growth rate segments (three total), fastener hole diameter, fastener hole edge distance, stress spectrum scale factor, and retardation parameter.

The probability density function (type and parameters) for each continuous random variable was determined through statistical metrics using the BestFit software program [35]. BestFit applied the chi-square, Kolmogorov–Smirnov, and Anderson–Darling tests to a set of data and compared the results from approximately 20 distribution types, for example, normal, lognormal, Weibull, logistic, extreme value, etc. The distributions were ranked according to the best fit to the data and the parameters for the distributions were determined. In addition, regression analysis using probability paper, that is, the Y axis was scaled according to a specific probability distribution, was performed and the R^2 value determined. An R^2 value near one indicates that the proposed probability distribution is a very good approximation for the data. Table 1 shows the mean and standard deviation, the coefficient of variation, the distribution type, and the R^2 value obtained from linear regression on distribution-specific probability paper.

The discrete variables were 1) the crack growth retardation model (Willenborg or Closure), 2) the geometry simplification assumption represented by the presence /absence of the countersink correction factor, and 3) the spectrum usage (NASA, SUPT, IFF).

A. Initial Flaw Size

Deterministic DTA is based on a rogue flaw size of 0.05 in. The rogue flaw size probability distribution was determined using T-38 wing teardown data from the −29 wing model fatigue test. At the end of the test, cracks from 23 wing fastener holes were grown backward in time to determine the equivalent initial flaw size distribution. The initial flaw size along the surface was modeled with a Weibull distribution, then offset by 0.04464 in. such that the mean of the distribution was 0.050 in., which is the assumption of a deterministic DTA. Figure 4 shows a probability plot of the data fit to a Weibull distribution as determined by BestFit. The distribution type is shown above the Y axis and listed in Table 1. The R^2 value is give at the top of the plot. A regression analysis of the data onto a Weibull probability scale revealed an R^2 value of 0.98.

B. Flaw Aspect Ratio

The flaw aspect ratio distribution was determined from the T-38 full-scale wing fatigue teardown data. An extreme value distribution was the best-fitting probability distribution. Figure 5 shows the comparison of the measured data to the extreme value distribution. A regression analysis of the data onto an extreme value probability scale revealed an R^2 value of 0.98.

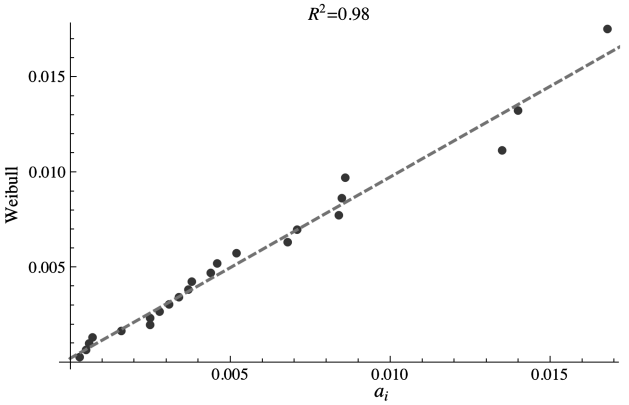

Fig. 4 Initial crack size.

C. Geometry Correction Factor

The variation in the geometry correction factor, beta, due to different stress intensity factor models was evaluated using three different geometry correction factor equations with identical geometry from three different well-established fatigue crack growth programs. Geometry correction factors were determined for a corner crack at a fastener hole in a wide plate using the AFGROW software [34], the Cracks98 Software [36], and the NASGRO software [32]. The results for 23 different crack lengths were then normalized by the AFGROW results, because AFGROW was the computer code used in this project, resulting in 69 data points. An extreme value distribution was the best fit to the normalized results. Figure 6 shows the comparison between the normalized beta factor and the extreme value distribution. A regression analysis of the data onto an extreme value probability scale revealed an R^2 value of 0.92.

D. Fastener Hole Diameter

The distribution for the fastener hole diameter was determined from 46 holes measured in a T-38 lower wing skin. The measurements were accurate to 0.005 in. Figure 7 shows a comparison of the data to a normal distribution fit to the data. A regression analysis of the data onto a normal probability scale revealed an R^2 value of 0.84. From Fig. 7, one can see that a finer resolution on the measurements would provide more confidence in the probability density function.

E. Fastener Hole Edge Distance

The fastener hole edge distance from the center of the hole to the part edge was based on 42 edge distance measurements made along the T-38 wing 15% spar on the left and right side of the wing. The data were best fit using a normal distribution. Figure 8 shows the probability plot. As can be seen in this figure, the data is in two groups,

Table 1 Random variable statistics and distribution type

Variable	Mean	Standard deviation	COV, %	Distribution
Initial rogue flaw size, in. (23 data pts.)	0.05	0.00456	9.11	Weibull offset 0.0446369 ($R^2 = 0.98$)
Crack aspect ratio (23 data pts.)	1.177	0.368	31.2	Extreme value ($R^2 = 0.98$)
Hole diameter, in. (46 data pts.)	0.260	0.000421	0.16	Normal ($R^2 = 0.84$)
Segment 1 crack growth rate C1 (61 data pts.)	5.92E-09	1.25E-09	21.2	Extreme value ($R^2 = 0.94$)
Segment 2 crack growth rate C2 (177 data pts.)	2.55E-10	6.07E-11	23.8	Extreme value ($R^2 = 0.97$)
Segment 3 crack growth rate C3 (210 data pts.)	4.20E-09	5.82E-10	13.8	Extreme value ($R^2 = 0.99$)
Hole edge distance, in. (42 data pts.)	0.897	2.42E-02	2.69	Normal ($R^2 = 0.90$)
Geometry correction factor (beta) (69 data pts.)	1.0095	0.0381	3.77	Extreme value ($R^2 = 0.92$)
Yield strength, ksi (15 data pts.)	62.0	3.65	5.88	Normal ($R^2 = 0.94$)
Plain strain fracture toughness, ksi root in. (11 data pts.)	33.6	1.25	3.73	Normal ($R^2 = 0.91$)
Thickness-dependent fracture toughness, ksi root in. (11 data pts.)	66.0	2.99	4.53	Normal ($R^2 = 0.86$)
IFF generalized Willenborg retardation parameter (5 data pts.)	2.59	0.220	8.52	Weibull ($R^2 = 0.81$)
IFF Closure model retardation parameter (5 data pts.)	0.334	0.0477	14.3	Extreme value ($R^2 = 0.91$)
SUPT generalized Willenborg retardation parameter (5 data pts.)	2.47	0.122	4.95	Weibull ($R^2 = 0.86$)
IFF stress spectrum scale factor (ksi) (1189 data pts.)	21.7	0.340	1.57	Normal ($R^2 = 0.95$)
SUPT stress spectrum scale factor (ksi) (1189 data pts.)	22.9	0.340	1.48	Normal ($R^2 = 0.95$)
NASA stress spectrum scale factor, ksi (1189 data pts.)	18.3	0.340	1.86	Normal ($R^2 = 0.95$)

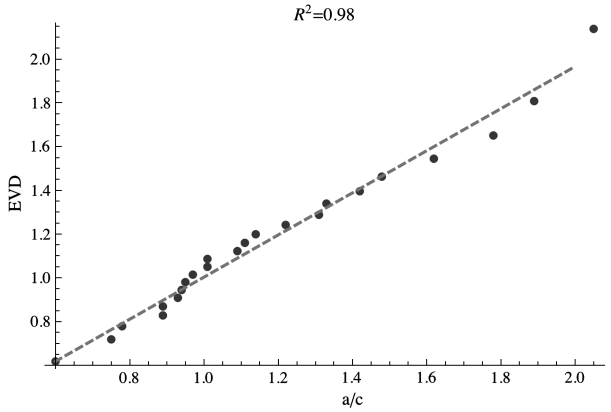

Fig. 5 Crack aspect ratio.

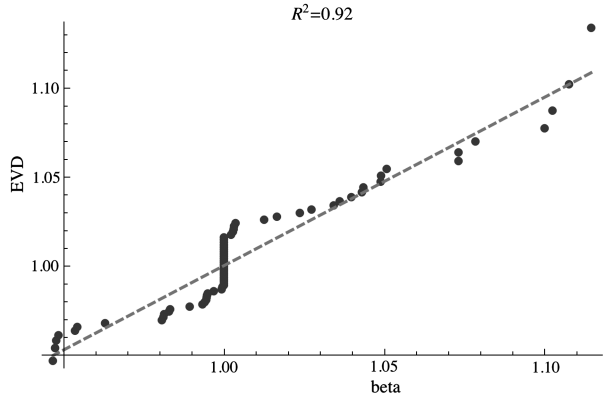

Fig. 6 Geometry correction factor (beta).

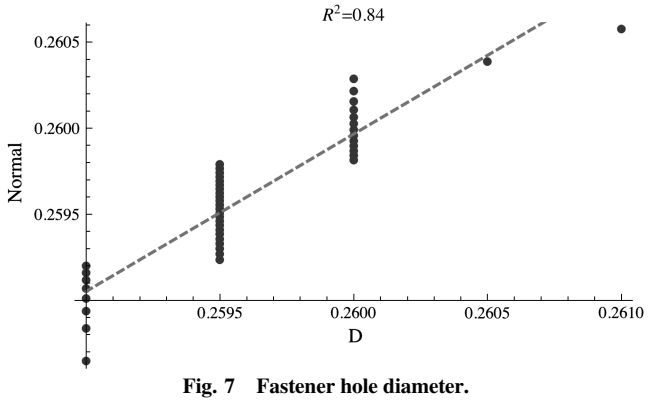

Fig. 7 Fastener hole diameter.

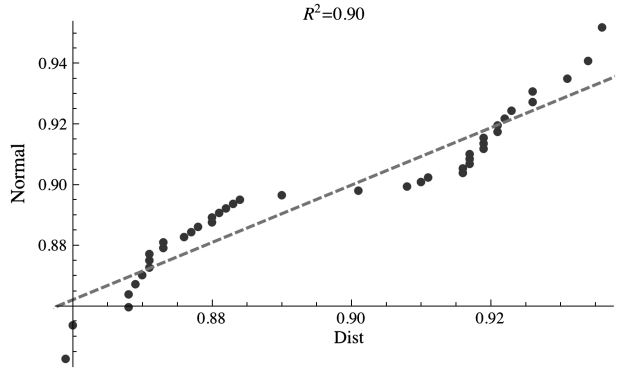

Fig. 8 Fastener hole edge distance.

corresponding to measurements made on the left or right side of the wing. This is expected because the wing fastener holes are hand drilled. Because the data were obtained from a single aircraft, it is anticipated that the left–right wing difference will average out. Thus, the data were not modeled as a bimodal PDF nor as two distinct PDFs. A regression analysis of the data onto a normal probability scale revealed an R^2 value of 0.90.

F. Yield Strength

The yield strength distribution was based on 15 tests. Figure 9 shows a comparison of the input data to a normal distribution. A regression analysis of the data onto a normal probability scale revealed an R^2 value of 0.94.

G. Plane Strain and Thickness-Dependent Fracture Toughness

The plane strain fracture toughness distribution was developed from 11 valid fracture toughness tests. Figure 10 shows a comparison of the test data to the normal distribution. Test data for thickness-dependent fracture toughness as a function of the material yield strength and plane strain fracture toughness were developed using Eq. (12). Figure 11 shows a comparison of the test data to the normal distribution. A regression analysis of the data onto a normal probability scale revealed an R^2 value of 0.91 for plane strain and an R^2 value of 0.86 for thickness-dependent fracture toughness.

H. Crack Growth Rate, Segments 1–3

The crack growth rate data used the results of the da/dN material tests. Figure 3 shows the da/dN versus ΔK test data for 448 test points at various R ratios collapsed using the Walker equation. Because there is a kink in the collapsed data, a three-segmented Walker equation was used. This resulted in distributions for the Paris constants within each segment of the Walker equation, C1, C2, and C3. The Paris exponent, n, was modeled as deterministic because it is well known that C and n are highly negatively correlated. An extreme value distribution was the best fit within each segment. R^2 values of

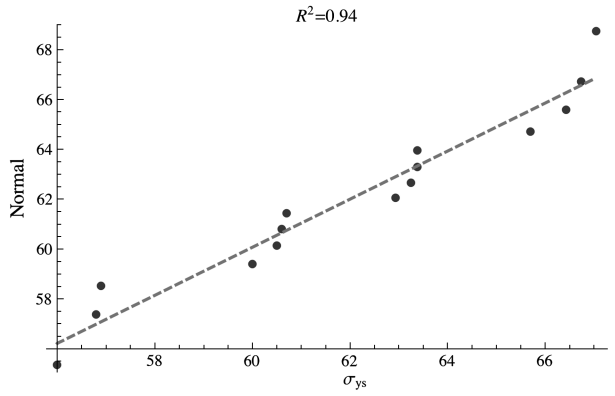

Fig. 9 Yield strength.

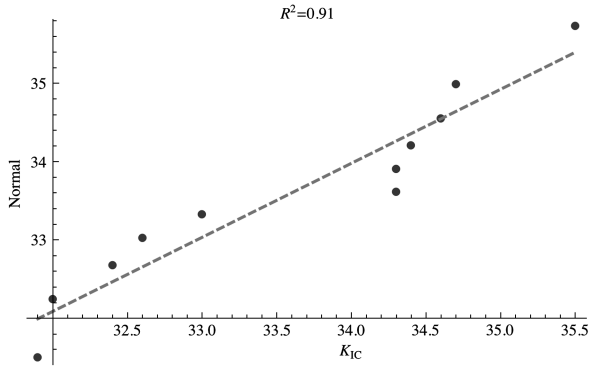

Fig. 10 Plane strain fracture toughness.

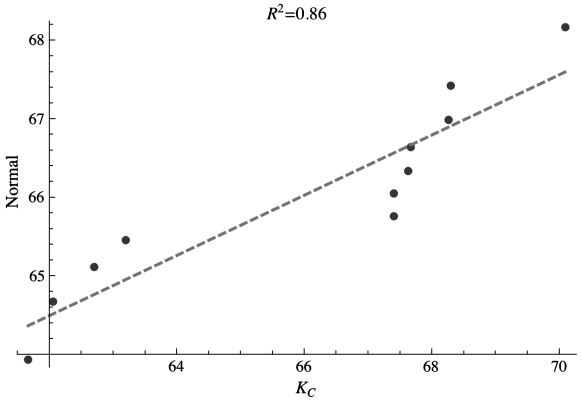

Fig. 11 Thickness-dependent fracture toughness.

0.94, 0.97, and 0.99 were obtained for the first, second, and third segments, respectively. Figures 12a–12c show the probability density functions for each segment.

I. Retardation Parameter

Retardation parameters were developed for two usages of this project, IFF [28] and SUPT.[‡] Parameter distributions for two different retardation models, generalized Willenborg and Closure, were developed for the IFF usage based on five coupon tests; see Figs. 13 and 14. IFF Willenborg was best fit with a Weibull distribution with $R^2 = 0.81$. IFF Closure was best fit with an extreme value distribution with $R^2 = 0.91$. A parameter distribution for the generalized Willenborg model was developed for the SUPT usage based on three coupon tests; see Fig. 15. The data were best fit with a Weibull distribution with $R^2 = 0.86$. The retardation value distributions are based on a very small set of test data and more test data would be more rigorous. However, as explained in Sec. VI, the probabilistic DTA results were not sensitive to the mean and standard deviation of the retardation parameters.

J. Stress Spectrum Scale Factor

The load-stress scale factor in AFGROW was used as a random variable to represent uncertainties in the stress at the FCL given a load value. To develop a stress-to-load ratio for the T-38 FCL A-15, 1189 flight measured strain gauge readings obtained from a DTA update program were used. The stress at this FCL was based on the wing bending moment at wing station 64.8. Based on a regression analysis of the strain gauge data, the standard deviation obtained was 0.34 ksi, which was used for each stress spectrum. The regression analysis of the data onto a normal probability scale revealed an R^2 value of 0.95.

IV. Probabilistic Sensitivity Analysis

Probabilistic sensitivity analyses were performed using a combination of the NESSUS® probabilistic analysis software [37] and the AFGROW fatigue crack growth analysis software [34]. The built-in AFGROW stress intensity factor solution for a single corner crack was used for the T-38 analysis; however, the probabilistic analysis approach employed is straightforward and can easily be used with the other fracture mechanics analysis models contained in AFGROW or other fatigue analysis programs.

Eight different Monte Carlo simulations were performed to compute probabilistic sensitivity factors for continuous variables and evaluate changes in the discrete variables (stress spectra, countersink correction factor idealization, and retardation model effects). Each simulation consisted of 5000 samples, that is, 5000 crack growth analysis runs, which is a sufficient number to obtain high confidence in the predicted sensitivities. The random variable sensitivities for each analysis were determined at the 50% probability level. That is, the sensitivity of the probability of failure with respect to the parameters of each random variable was determined when the probability of failure was 50%. A probability of failure of 50% was chosen because a rogue flaw size of 0.05 as specified in the DTA is already a rare event, for example, one in a million.

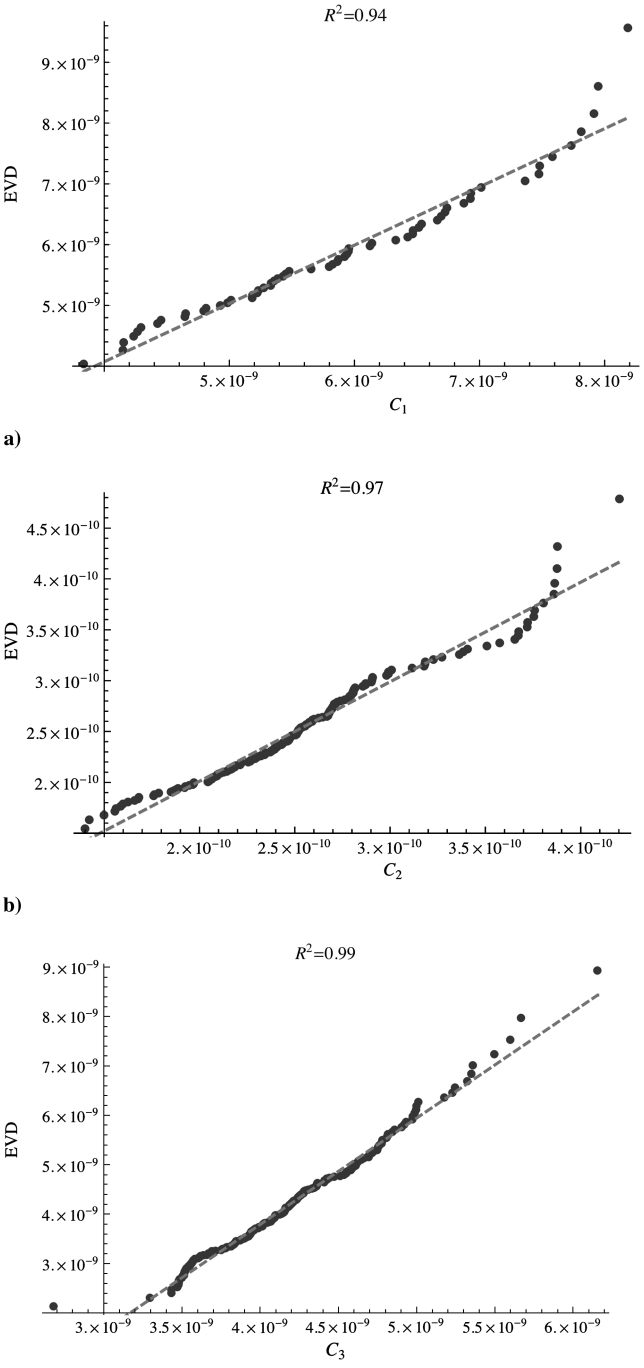

Fig. 12 Crack growth rate data: a) crack growth rate (segment 1), b) crack growth rate data (segment 2), c) crack growth rate data (segment 3).

Simulations were performed with and without the countersink correction factor for each usage (IFF, SUPT, NASA). Simulations for the IFF usage used both the Willenborg and Closure retardation models; the simulation for the SUPT usage used the Willenborg retardation model; and simulations for the NASA usage were assumed to be unretarded because it is so mild. The computed mean, standard deviation, and coefficient of variation results (COV= standard deviation/mean) for the eight Monte Carlo simulations are given in Table 2. To ensure a small sampling variance, 5000 samples were sufficient. For example, the 95% lower and upper confidence bounds for the IFF usage with countersink mean value are 3288 and 3332 cycles, respectively, and the 95% confidence limits for the

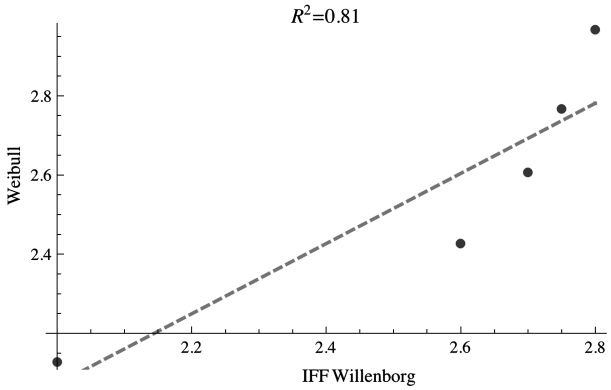

Fig. 13 IFF generalized Willenborg retardation parameter.

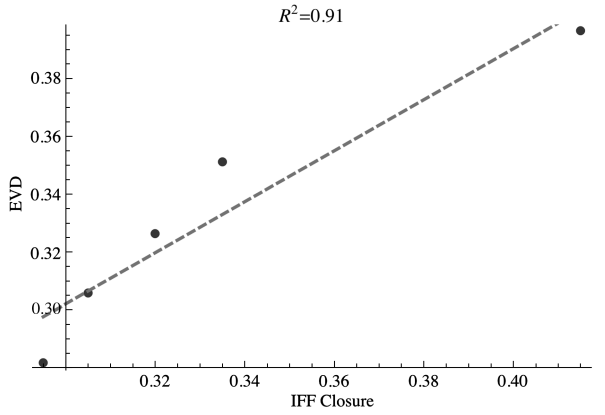

Fig. 14 IFF Closure retardation parameter.

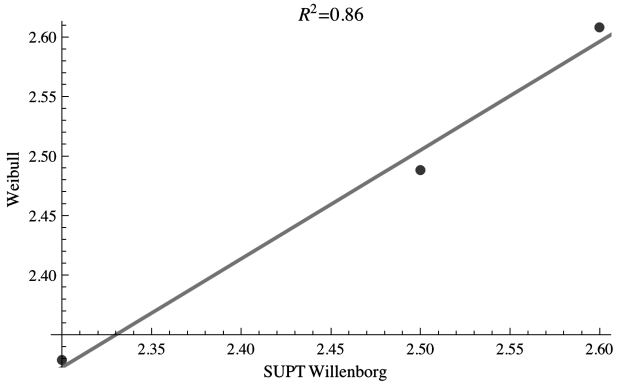

Fig. 15 SUPT generalized Willenborg retardation parameter.

standard deviation are 777 and 808, respectively. Similar results are obtained for the other quantities in the table. Variance estimates indicate that coefficient of variation of the probabilistic sensitivities due to the application of limited sampling (5000 samples) yields values of a few percent, for example, $\mathrm{COV}_{\mu\mathrm{HoleDiameter}} \sim 2\%$ and $\mathrm{COV}_{\mu\mathrm{beta}} \sim .4\%$. Thus, sufficient samples have been applied to provide confidence in the probabilistic sensitivity results.

From the mean and standard deviation of the flight hours until failure listed in Table 2, the results indicate the importance of including the countersink correction factor in the crack growth analysis (compare runs 1 and 3, 2 and 4, 5 and 6, and 7 and 8). There is about a 40% decrease in life when the countersink is modeled. In addition, the standard deviation of life is significantly different. Therefore, the probability of failure will be significantly affected by the inclusion of the countersink correction factor. It is interesting to note that the coefficient of variation is nearly constant for the same countersink model (compare runs 1 and 2 and 5 and 7, and 3 and 4).

The choice of retardation model does not significantly affect the mean and standard deviation results (compare runs 1 and 2, and 3 and 4) and, therefore, will not significantly affect the probability of failure. The usage of course affects the mean and standard deviation but the question is whether the relative ranking of the continuous random variables changes as a function of the usage; this assumption is checked later (see Table 6).

Table 3 shows the sensitivity results ($\Gamma_{\mu_i}, \Gamma_{\sigma_i}, \hat{S}_{\mu_i}, \hat{S}_{\sigma_i}, S^2_{\mu_i} S^2_{\sigma_i}$) for the most severe case of IFF usage with the countersink modeled, and the Willenborg retardation model. Values of $S^2_{\mu_i}$ and $S^2_{\sigma_i}$ below 2% have been omitted to highlight the important parameters. Results for Γ_{μ_i} and Γ_{σ_i} have inverse units of the random variable, forexamplee, units for Γ_{μ_i} and Γ_{σ_i} of the initial flaw size are inches^{-1}. Indices $\hat{S}_{\mu_i}$, $\hat{S}_{\sigma_i}$, $S^2_{\mu_i}$, and $S^2_{\sigma_i}$ are nondimensional. The results for $S^2_{\mu_i}$ indicate that, with respect to variations in the mean values, the hole diameter (negative sensitivity), beta geometry correction factor (positive), and the stress modeling error (positive) comprise 95% of the total sensitivity with the hole diameter dominant. The index $\hat{S}_{\mu_i}$ can be used to predict the percent decrease in the POF for a percent increase in the mean hole diameter. For example, a 1% increase in the mean value of the hole diameter would lead to a decrease in the probability of failure of approximately 0.117, for example,

$$\begin{aligned}\Delta P_f &\approx \frac{\partial P_f}{\partial \mu_{\mathrm{Diam}}}(0.01)\mu_{\mathrm{Diam}} = (0.01)\hat{S}_{\mathrm{Diam}} \\ &= (0.01)(-11.7) = -0.117\end{aligned} \tag{14}$$

The results for $S^2_{\sigma_i}$ indicate that, with respect to variations in the standard deviations, the third segment of the $\mathrm{d}a/\mathrm{d}N$ fatigue crack growth rate (C3) (positive), the geometry correction factor (positive), and the initial flaw aspect ratio (negative) comprise 86% of the sensitivity. The negative sensitivity of the POF with respect to the standard deviation of the initial crack size aspect ratio occurs because the POF is approximately 50%. The flaw shape (aspect ratio) has a larger effect than the initial flaw size because a crack with a large aspect ratio is more likely to grow into the more severe case of a through crack. The POF is significantly more sensitive to variations in the mean values of the parameters rather than the standard deviations. For example, a 1% reduction in the standard deviation of C3 will result in a 0.27% reduction in POF. However, it may be easier to control the variation in a parameter and, hence, to reduce the standard deviation.

Table 2 Flight hours to failure results (5000 samples per analysis)

Run no.	Usage	Retardation model	Countersink	Mean (flight hours)	Standard deviation (flight hours)	COV
1	IFF	Willenborg	Yes	3310	793	0.24
2	IFF	Closure	Yes	3341	948	0.28
3	IFF	Willenborg	No	5504	2331	0.42
4	IFF	Closure	No	5840	2818	0.48
5	SUPT	Willenborg	Yes	15226	3509	0.23
6	SUPT	Willenborg	No	23687	9082	0.38
7	NASA	None	Yes	93870	21393	0.23
8	NASA	None	No	166219	81827	0.49

Table 3 Sensitivity results for T-38: IFF usage, countersink model, Willenborg retardation

	Γ_μ	Γ_σ	$\hat{S}_\mu$	$\hat{S}_\sigma$	S_μ^2	S_σ^2
Initial rogue flaw size	1.16E + 01	−5.83E + 00	0.58	−0.03	——	——
Crack aspect ratio	4.37E − 01	−1.88E − 01	0.52	−0.07	——	0.24
Hole diameter	−4.50E + 01	3.75E + 01	−11.7	0.02	0.64	——
Crack growth rate C1	2.59E + 07	−2.42E + 06	0.15	0.00	——	——
Crack growth rate C2	5.83E + 08	−1.73E + 08	0.15	−0.01	——	——
Crack growth rate C3	4.65E + 08	1.44E + 08	1.96	0.08	——	0.35
Hole edge distance	−2.03E + 00	−1.97E + 01	−1.82	0.00	——	——
Geometry correction factor	5.72E + 00	1.94E + 00	5.77	0.07	0.16	0.27
Yield strength	−1.11E − 03	−6.56E + 04	−0.07	0.00	——	——
Plain strain fracture toughness	1.23E − 02	−1.88E + 02	0.41	−0.02	——	——
Plain strain fracture toughness	1.54E − 03	−7.08E + 03	0.10	−0.02	——	——
IFF stress spectrum scale factor	2.57E − 01	−6.88E + 03	5.57	0.00	0.15	——
Retardation parameter	7.68E − 01	−1.29E + 03	1.99	−0.03	——	——

V. Effect of Discrete Variables

A. Countersink

As shown in Table 2, the modeling of the countersink has a significant effect on the mean and standard deviation of the flight hours to failure and, by extrapolation, the POF. However, it remains to be determined whether the relative importance of the continuous variables changes if the countersink is modeled or not. The comparison index χ can be used to answer this question. Table 4 shows the comparison indices (χ_μ, χ_σ) for four different analyses modeled with and without the countersink, for example, $\chi_\mu = \bar{S}_\mu^{\text{Countersink}} \bullet \bar{S}_\mu^{\text{No Countersink}}$. The results indicate that, in all cases, the comparison indices with respect to the mean are very close to 1, indicating that modeling the countersink does not change the relative sensitivities with respect to the mean values. Therefore, the conclusions obtained from the analysis results shown in Table 3 are reliable.

Table 4 does, however, indicate that modeling the countersink has a significant impact on the relative importance with respect to the standard deviations. For IFF and SUPT usage, the comparison indices were 0.64 and 0.60, respectively, indicating some change. If the countersink was modeled, the significant variables were C3, beta, and the initial flaw aspect ratio. If the countersink was not modeled, the significant variables were C3, beta, the initial flaw aspect ratio, fracture toughness (plane stress and strain), and the retardation factor, that is, two additional variables were significant.

For NASA usage, the comparison index is approximately zero. This is primarily due to the change in sign of S_σ for the initial crack size aspect ratio. If the countersink is modeled, S_σ is negative and an increase in the standard deviation will decrease the probability of failure, whereas if the countersink is not modeled, S_σ is positive. Thus, modeling the countersink has a very significant affect on the sensitivities of the continuous variables in this case.

In summary, the sensitivities of the POF with respect to the mean for the continuous variables do not change if the countersink correction factor is modeled. However, sensitivities of the POF with respect to the standard deviation is affected, moderately so for the IFF and SUPT usages and significantly so for the NASA usage.

B. Retardation Model

The effect for the retardation model, Willenborg or Closure, has minimal effect on the mean and standard deviation of the flight hours to failure; see Table 2, runs 1 and 2 and 3 and 4. The comparison indices for the IFF usage, with and without the countersink modeled, are very similar for the Closure and Willenborg retardation models. The comparison indices with respect to the retardation model are shown in Table 5. These results reinforce that the choice of retardation model does not significantly affect the probability of failure nor does it affect relative sensitivities of the continuous variables provided properly calibrated retardation constants are used.

C. Usage

Clearly the usage, severe to mild, will affect the mean flight hours to failure, as shown in Table 2 (compare runs 1 and 5 and 7). The comparison indices are listed in Table 6. Little change was seen in (χ_μ or χ_σ) when comparing IFF and SUPT whether or not the countersink was modeled. However, as discussed earlier with respect to the countersink modeling issue, comparisons of either IFF or SUPT with the NASA usage indicate a change in the random variable rankings.

VI. Discussion

The probabilistic sensitivities are clearly problem dependent and will vary based upon the model and numerical values used. However, the methodology is generic and can be used with any fatigue model or input data. Other typical scenarios could include a different FCL, a different aircraft such as a transport, or a different probability level about which to compute the sensitivities. The approach presented here was to analyze an aircraft structural location as realistically as possible using data from material tests and teardowns. Keeping the data and model-dependent nature of the conclusions in mind, some comparisons with other studies are useful.

The DTA considered here was more comprehensive, considering more variables and expected variations in the variables, than that by

Table 4 Countersink modeling comparison indices with respect to mean (χ_μ) and standard deviation (χ_σ) for results with and without countersink

Analyses	χ_μ	χ_σ
IFF usage, Willenborg retardation	0.99	0.64
IFF usage, Closure retardation	0.97	0.64
SUPT usage, Willenborg retardation	0.99	0.60
NASA usage, no retardation	0.95	0.00

Table 5 Retardation parameter modeling comparison indices with respect to mean (χ_μ) and standard deviation (χ_σ) (comparison of Willenborg vs Closure)

Analyses	χ_μ	χ_σ
IFF usage, with countersink	0.94	0.97
IFF usage, without countersink	0.95	0.94

Table 6 Comparison indices for usage

Usages	Countersink	Retardation	χ_μ	χ_σ
IFF vs SUPT	Yes	Willenborg/Willenborg	0.99	0.98
IFF vs NASA	Yes	Willenborg/none	0.68	0.82
SUPT vs NASA	Yes	Willenborg/none	0.67	0.85
IFF vs SUPT	No	Willenborg/Willenborg	0.99	0.99
IFF vs NASA	No	Willenborg/none	0.47	0.59
SUPT vs NASA	No	Willenborg/none	0.32	0.55

McGinty [14]. However, in both studies the importance of the geometry correction factor was borne out. McGinty identified the Paris exponent crack growth rate as an important parameter. In our research, the Paris constant was modeled as a random variable and was identified as important but not dominant; the standard deviation of the Paris constant in the large crack growth regime was one of three important variables. The variation of the Paris constant in the other two regions was insignificant.

Fawaz and Harter [15] identified the initial flaw size assumption, geometry correction factor, load interaction models, crack growth rate data, and stress intensity factor as first-order effects. Our research determined that the mean hole diameter was a dominant factor that was not explicitly considered as a parameter by Fawaz and Harter. Both studies identified the geometry correction factor as significant. The initial flaw size aspect ratio was significant in our results, not the initial crack size. The crack growth rate standard deviation was significant in our work but only in the larger crack growth region. The retardation model used in our study, Willenborg vs Closure, showed minimal impact in contrast to Fawaz and Harter, which showed a significant difference in cycles to failure between the Harter, Wheeler, and Willenborg retardation models. Extension of this research to the Harter and Wheeler models may warrant further investigation.

In probabilistic analysis, characterizing the statistics and probability distribution is often challenging. However, in many cases, the probabilistic sensitivity method employed is robust to distribution type. For example, it is known that probabilistic sensitivities are invariant to distribution type when computing sensitivities of the mean or standard deviation of the response (cycles to failure) if the input and outputs can be modeled by a quadratic (or linear) relationship. In this example, the quadratic model is a good approximation ($R^2 = 0.91$); therefore, the rankings using probabilistic sensitivities of the median as a metric should be largely insensitive to the type of probability distribution, for example, normal vs Weibull, given the same mean and standard deviation for the input variables. Thus, the results would not change significantly if a normal distribution was used instead of an extreme value distribution keeping the mean and standard deviation the same. Because in the T-38 example problem the input and output relationship is well modeled by a quadratic approximation, and the median ($P = 0.5$) is close to the mean, the probabilistic sensitivity results are concluded to be robust to the random variable distributions.

VII. Conclusions

This research employed a probabilistic sensitivity analysis method that explicitly computed the partial derivative of the probability of failure with respect to the mean and standard deviation of the input parameters. The methodology is attractive for a variety of reasons: 1) it explicitly considers the variance of the model parameters, 2) it can be employed with any complexity of deterministic model, and 3) the sensitivities are obtained for negligible additional computational cost.

The methodology was applied to a probabilistic damage tolerance analysis of a T-38 lower wing fastener hole. Probability distributions from test data were determined for 13 continuous random variables. A total of eight T-38 simulations were performed to assess the affect of discrete variables with each simulation consisting of 5000 Monte Carlo samples with 13 random variables analyzed for each simulation. The T-38 FCL was analyzed with and without countersink correction factors, with three different usages, and two different retardation models for the IFF and SUPT usages.

The probabilistic sensitivity results indicate that the POF was sensitive to the fastener hole diameter, the geometry correction factor (beta), the crack growth rate at higher ΔK (C3), and the stress spectrum scale factor. Of these variables, only the geometry correction factor was sensitive to variation in both the mean and standard deviation. Combining this fact with the observation that including the countersink geometry correction factor makes a large difference in life, an accurate geometry correction factor is critical. This result maybe surprising when considering that the coefficient of variation of beta was only 3.8%. Even with a small variation, beta is an important variable.

The POF was sensitive to the fastener hole diameter mean value but not its standard deviation. This would indicate that during the design process selecting the fastener hole diameter is critical but the typical manufacturing fastener hole diameter variation is acceptable from a damage tolerance perspective. The POF is not sensitive to the edge distance. The results are also sensitive to the mean value of the stress spectra scale factor but not its standard deviation. This is not surprising given that controlling the far-field stress in a critical element of designing fatigue-resistant parts. The results are sensitive to the standard deviation of the crack growth rate in the higher ΔK range. This would indicate that better process control in the material-manufacturing phase should reduce the scatter in damage tolerance life estimates.

The POF was sensitive to the crack aspect ratio standard deviation but not the initial flaw size. This is likely due to the fact that a through crack is more severe than a corner crack. Thus, shorter cracks with large aspect ratios, which are nearly through cracks, can be more severe than longer cracks with small aspect ratios, which are still very much corner cracks.

The simulation results and sensitivities are very similar for the two different retardation models. This indicates that the choice of retardation model is not a key analysis driver, as long as the retardation parameter is calibrated to test data.

It is interesting that the results are not sensitive to the material yield strength or either of the fracture toughness values. These values all affect the critical crack length. The fact that they are not critical indicates that for this FCL critical crack length is not important in calculating the total life of the part. Reviewing the DTA crack growth curve for this FCL indicates that the crack is growing nearly vertically at the end of its life so that a large change in critical crack length does not translate into a large change in crack growth life.

When considering potential design changes, one would, of course, factor in the level of effort, for example, cost, to implement the change. In this case, changing the mean diameter of the hole would most likely be straightforward to accomplish. Changing the mean error in the geometry correction factor may require research funding into improved stress intensity solutions.

The results obtained through a PDTA will, of course, depend upon the FCL considered and the data for deterministic and probabilistic inputs. Our results and conclusions are based on a T-38 analysis. Profitable future research would consist of a similar study on another aircraft or FCL.

In summary, a probabilistic sensitivity method was presented and applied to a detailed probabilistically based damage tolerance analysis of a fatigue critical location of a T-38. The sensitivity results were used to ascertain the relative importance of the inputs to a DTA. As much as possible, realistic data were used to determine the correct random variable distributions. The results indicate that, predominately, the fastener hole diameter, the geometry correction factor (beta), the crack growth rate at higher ΔK values (C3), and the stress spectrum scale factor are the important factors to characterize and perhaps improve to obtain more accurate DTA estimates.

Acknowledgments

The authors would like to recognize the following people for their contributions to this effort: Clair Paul for conceiving of this project, and Arvind Nagar for managing and providing technical direction for this project. Both are from the U.S. Air Force Research Laboratory. We would also like to thank Kurt Rabideau, the T-38 Aircraft Structural Integrity Program manager at the time of this study, for providing technical assistance and data. This paper was cleared for public release on 09 September 2009 as case 88ABW-2009-3945.

References

[1] Skinn, D. A., Gallagher, J. P., Berens, A. P., Huber, P. D., and Smith, J., "Damage Tolerant Design Handbook," U.S. Air Force Materials Directorate, WL-TR-94-4052, May 1994.

[2] Yang, J. N., "Statistical Estimation of Service Cracks and Maintenance Cost for Aircraft Structures," *Journal of Aircraft*, Vol. 13, No. 12, Dec. 1976, pp. 929–937. doi:10.2514/3.58732

[3] Yang, J. N. and Manning, S. D., "Stochastic Crack Growth Analysis Methodologies for Metallic Structures," *Engineering Fracture Mechanics*, Vol. 37, 1990, pp 1105–1124. doi:10.1016/0013-7944(90)90032-C

[4] Yang, J. N. and Manning, S. D., "Aircraft Fleet Maintenance based on Structural Reliability Analysis," *Journal of Aircraft*, Vol. 31, 1994, pp 419–425. doi:10.2514/3.46502

[5] Yang, J. N. and Manning, S. D., "A Simple Second Order Approximation for Stochastic Crack Growth Analysis," *Engineering Fracture Mechanics*, Vol. 53, No. 5, 1996, pp 677–686. doi:10.1016/0013-7944(95)00130-1

[6] Lincoln, J. W., "Risk Assessment of an Aging Military Aircraft," *Journal of Aircraft*, Vol. 22, No. 8, 1985, pp 687–691. doi:10.2514/3.45187

[7] Lincoln, J. W., "Risk Assessments—USAF Experience," *Durability of Metal Aircraft Structures—Proceedings on the International Workshop on Structural Integrity of Aging Airplanes*, Atlanta Technology Publication, Atlanta, 1992, pp 244–257.

[8] Berens, A. P., Hovey, P. W., and Skinn, D. A., "Risk Analysis for Aging Aircraft Fleets," Flight Dynamics Directorate, Wright Laboratory, Air Force Systems Command, WL-TR-91-3066, Wright–Patterson Air Force Base, OH, 1991.

[9] Berens, A. P., and Loomis, J. S., "Update of the PROF Computer Program for Aging Aircraft Risk Analysis," Univ. of Dayton Research Inst., F09603-95-D-0175, Nov. 1998.

[10] Miedlar, P. C., Berens, A. P., Hovey, P. W., Boehnlein, T. R., and Loomis, J. S., "PRoF v3 PRobability Of Fracture," Univ. of Dayton Research Inst., F09650-03-D-0001, Dec. 2005.

[11] Cardinal, J. W., Burnside, H., Sparks, W., and Schrader, K., "Risk and Economic Implications of DADTA for Foreign Military Operators of Non-USAF Fleets," *Proceedings of the 1999 International Conference on Aircraft Fatigue*, Vol. 1, July 1999, pp. 553–576.

[12] Shi, P., and Mahadevan, S., "Damage Tolerance Approach for Probabilistic Pitting Corrosion Fatigue Life Prediction," *Engineering Fracture Mechanics*, Vol. 68, No. 13, Sept. 2001, pp. 1493–1507. doi:10.1016/S0013-7944(01)00041-8

[13] Rusk, D. T., Kuen, Y. L., Swartz, D. D., and Ridgeway, G. K., "Bayesian Updating of Damage Size Probabilities for Aircraft Structural Life-Cycle Management," *Journal of Aircraft*, Vol. 39, No. 4, July/Aug. 2002, pp. 689–696. doi:10.2514/2.2983

[14] McGinty, R. D., "Sensitivity of Fatigue Crack Growth Rates to Operating Conditions, Sample Problem No. MERC-3," *USAF Damage Tolerant Design Handbook: Guidelines for the Analysis and Design of Damage Tolerant Aircraft Structures*, edited by P. C. Miedlar, A. P. Berens, A. W. Gunderson, and J. P. Gallagher, U.S. Air Force, AFRL-VA-WP-TR-2003-3002, Wright–Patterson Air Force Base, OH, Nov. 2002.

[15] Fawaz, S. A., and Harter, J. A., "Impact of Parameter Accuracy on Aircraft Structural Integrity Estimates," U.S. Air Force, AFRL-VA-WPTR-2001-3057, 2001.

[16] Evans, M., Hastings, N., and B. Peacock, *Statistical Distributions*, 3rd ed., Wiley, Hoboken, NJ, 2000.

[17] Devore, J. L. *Probability and Statistics for the Engineering and the Sciences*, 6th ed, Thomson, Brooks/Cole, Belmont, CA, 2004.

[18] Ayyub, B. M., and McCuen, R. H., *Probability, Statistics, & Reliability for Engineers*, CRC Press, Boca Raton, FL, 1997.

[19] Anderson, T. W., and Darling, D. A., "Asymptotic Theory of Certain "Goodness of Fit" Criteria Based on Stochastic Processes," *Annals of Mathematical Statistics*, Vol. 23, pp. 193–212. doi:10.1214/aoms/1177729437

[20] Rubinstein, R. Y., and Kroese, D. P., *Simulation and the Monte Carlo Method*, 2nd ed., Wiley-Interscience, New York, 2007.

[21] Melchers, R. E., *Structural Reliability Analysis and Prediction*, 2nd ed., Wiley, New York, 1999.

[22] Wu, Y.-T., Millwater, H. R., and Cruse, T. A., "Advanced Probabilistic Structural Analysis Method for Implicit Performance Functions," *AIAA Journal*, Vol. 28, No. 9, Sept. 1990, pp. 1663–1669. doi:10.2514/3.25266

[23] Ang, A. H.-S., and Tang, W. H., *Probability Concepts in Engineering Planning and Design*, 2nd ed., Vol. 1, Wiley, New York, 2006.

[24] Karamchandani, A. K., "New Methods in Systems Reliability," Ph.D. Dissertation, Stanford Univ., Palo Alto, CA, 1990.

[25] Rubinstein, R. Y., and Shapiro, A., *Discrete Event Systems, Sensitivity Analysis and Stochastic Optimization by the Score Function Method*, Wiley, Chichester, England, U.K., 1993.

[26] Millwater, H. R., "Universal Properties of Kernel Functions for Probabilistic Sensitivity Analysis," *Probabilistic Engineering Mechanics*, Vol. 24, 2009, pp. 89–99. doi:10.1016/j.probengmech.2008.01.005

[27] "Usage and Preliminary Damage Tolerance Assessment Report for the National Aeronautics and Space Administration T-38A," Southwest Research Inst., Project Number 06-6927, San Antonio, TX, April 1996.

[28] "Usage Assessment Report, AETC AT-38B Introduction to Fighter Fundamentals Pilot Training," Southwest Research Inst., Project Number 06-6723, San Antonio, TX, May 1997.

[29] "F-5 FMS Durability and Damage Tolerance Update Revised Final DADTA Report—F-5E/F, Republic of Korea Air Force," Southwest Research Inst., Project Number 06-4222, San Antonio, TX, May 1996.

[30] "T-38 -29 Wing Fatigue Critical Area Coupon Testing," Southwest Research Inst., Project Number 7562/9, Final Report: Coupon and Additional Testing, San Antonio, TX, Sept. 1984.

[31] "T-38 SUPT/IFF Coupon Analysis Results," Southwest Research Inst., Project Number 18-1334, San Antonio, TX, March 2001.

[32] "NASGRO™ Fracture Mechanics and Fatigue Crack Growth Analysis Software," Version 4.02, NASA Johnson Space Center and Southwest Research Institute, Sept. 2002.

[33] Willenborg, J., Engle, R. M., Jr., and Wood, R. A., "A Crack Growth Retardation Model Using an Effective Stress Concept," AFFDL-TM-71-1-FBR, Wright–Patterson Air Force Base, OH, 1971.

[34] AFGROW Version 4.0005.12.10, U.S. Air Force/Air Force Research Laboratory/Air Vehicles Directorate, July 2002, http://www.afgrow.net.

[35] BestFit Version 4.0, Palisade Corporation, Copyright 2000.

[36] Miedlar, P. C., and Gallahher, J. P., *Cracks98 System User's Manual*, Univ. of Dayton Research Inst., Dayton OH, April 1998.

[37] Thacker, B. H., Riha, D. S., Fitch, S. H. K., Huyse, L. J., and Pleming, J. B. "Probabilistic Engineering Analysis Using the NESSUS Software," *Structural Safety*, Vol. 28, Nos. 1–2, Structural Reliability Software, Jan.–April 2006, pp. 83–107. doi:10.1016/j.strusafe.2004.11.003